1100–1107 *Nucleic Acids Research, 1997, Vol. 25, No. 6*

Parallel-stranded linear homoduplexes of d(A$^+$-G)$_{n > 10}$ and d(A-G)$_{n > 10}$ manifesting the contrasting ionic strength sensitivities of poly(A$^+$·A$^+$) and DNA

Nina G. Dolinnaya, Aylin Ulku and Jacques R. Fresco*

Department of Molecular Biology, Princeton University, Princeton, NJ 08544-1014, USA

Received January 8, 1997; Accepted January 22, 1997

ABSTRACT

In contrast to shorter homologs which only form a single-stranded nucleic acid α-helix in acid solution at [Na$^+$] ≤ 0.02 M Na$^+$, d(A-G)$_{20,30}$ form *in addition* a parallel-stranded duplex with (A$^+$·A$^+$) and (G·G) base pairs and interstrand dA$^+$···PO$_2^-$ ionic and dA$^+$NH$_2$···O=P H-bonds. Under conditions where duplex prevails over α-helix, the contribution of the base–backbone interactions to stability varies directly with [H$^+$] and inversely with [Na$^+$], just as in poly(A$^+$·A$^+$). These duplexes are characterized by intense circular dichroism and a large cooperative thermally-induced hyperchromic transition that is dependent on oligomer concentration. Dimethylsulfate reactivity of the dG residues indicates G·G and therefore dA$^+$·dA$^+$ rather than dA$^+$·G base pairs. At much higher ionic strength (Na$^+$ ≥ 0.2 M) the protonated base–backbone interactions are so weakened that duplex stability becomes increasingly dependent upon H-bonded base pairing and stacking and almost independent of pH. Between pH 6 and 8 this duplex structure is devoid of protonated dA residues and shows positive dependence of T_m on ionic strength similar to that of DNA.

INTRODUCTION

Repeating homopurine–homopyrimidine sequences adopt a variety of unique structures to relieve superhelical stress (1,2). In upstream gene control elements such sequences also serve as sites of protein binding not to the DNA duplex itself, but rather to some conformational variant of one of the strands (3,4). It is probably for this reason that a number of studies have focused on the alternating homopurine sequence d(A-G)$_n$. This sequence forms a broad spectrum of conformations under different pH and ionic conditions, including parallel-stranded duplexes (5,6), a hairpin duplex (7–9), a two-hairpin tetraplex (7,10) and a novel type of single-stranded helix (11–14). The latter conformation, which has been observed for d(A-G)$_6$ and d(A-G)$_{10}$ in an acidic milieu at low ionic strength, is stabilized not by helically wound stacks of bases or base pairs, but by an unusual combination of ionic and hydrogen (H-) bonds between dA$^+$ residues and the phosphodiester backbone such that the dA residues do not overlap their dG nearest neighbors. This structure, referred to as the (nucleic acid) α-helix, occurs below pH 6 in 0.01 M Na$^+$, reaches maximum stability at pH 4 and is characterized by intense circular dichroism and minor hypochromicity. The pK_a for the acid-induced transition of d(A-G)$_{10}$ to d(A$^+$-G)$_{10}$ in 0.01 M Na$^+$ is 5.3 at 25°C and increases with lower temperature and lower Na$^+$ concentration. The ionic interactions that maintain the α-helix are characteristically very sensitive to cation concentration because shielding of the phosphate groups weakens the ionic and associated H-bonds that stabilize the structure.

Increasing the length of d(A-G)$_n$ from n = 6 to n = 10 raises the pK_a of the coil to α-helix transition (12). If this trend were to continue as the number of d(A-G) repeats is increased, it is conceivable that the longer lengths found in mammalian gene control elements would have pK_a values within the physiological pH range. To determine if this is so, we examined the solution properties of the structures formed by d(A-G)$_{20}$ and d(A-G)$_{30}$ under varying conditions of pH and ionic strength. We thereby identified two related double-stranded helical structures formed by these oligomers but not by d(A-G)$_{10}$. Between 0.001 and 0.01 M Na$^+$ below pH 6.0, both oligomers form an acid-dependent parallel-stranded duplex with A$^+$·A$^+$ and G·G base pairs. Nevertheless, this structure is stabilized primarily by ionic and H-bonds between the protonated dA residues and the backbone phosphates of opposing strands, since its stability increases upon lowering either ionic strength or the dielectric constant of the medium. Under slightly more acidic conditions, these duplexes are in equilibrium with the single-stranded α-helix previously described for d(A$^+$-G)$_{6,10}$ (11–14). At Na$^+$ ≥ 0.21 M above pH 3.5, the ionic and associated H-bonds between dA$^+$ and the backbone in the linear duplexes of d(A-G)$_{20,30}$ are suppressed. While the basic duplex structure is retained, it is now stabilized principally by helically wound and stacked A·A and G·G base pairs, for the counterion shielding now reduces interstrand backbone repulsion. As a consequence, the strong pH-dependence of stability evident at low ionic strength essentially disappears and the duplex even exists above neutral pH. As noted, in these higher Na$^+$ concentrations the single-stranded α-helix does not occur at any pH or strand length.

*To whom correspondence should be addressed. Tel: +1 609 258 3927; Fax: +1 609 258 6730; Email: jrfresco@princeton.edu

MATERIALS AND METHODS

Oligonucleotides

$d(A\text{-}G)_{20}$ and $d(A\text{-}G)_{30}$ were synthesized by the phosphoramidite method, deprotected, purified by 8 or 6% denaturing PAGE and their bands eluted and desalted by reverse-phase chromatography (11). Oligomer concentrations (*c*) were determined spectrophotometrically and are reported on a residue basis. Purity was confirmed by denaturing PAGE of 5′-^{32}P-labeled oligomers. ε_{260} per residue of $d(A\text{-}G)_{20}$ and $d(A\text{-}G)_{30}$ were assumed to be 9500 in distilled water, the same as for $d(A\text{-}G)_{10}$ and poly[d(A-G)] (15). The deoxyoligomers 5′-CACCTGACTCCTGTGGAGAAGTCTGCCGTTACTGCCCTGTG-3′ (41mer) and 5′-CTGACTCCTGTGGAGAAGTCTGCCGTTACTGCCCT-3′ (35mer) and their complementary strands were synthesized by the phosphoramidite method and purified as above.

Solvents

Aqueous buffers between pH 3.5 and 6.0 ± 0.05 were prepared by titrating sodium acetate with acetic acid to a final Na^+ concentration of 0.01 M. Aliquots of these buffers were also diluted appropriately with H_2O or near-saturated NaCl to achieve 0.001 M and 0.21 M Na^+ and their pH values redetermined. pH measurements were made with a Radiometer pH meter 26 and a glass pH microelectrode standardized with an appropriate buffer at room temperature and at 4°C.

CD spectroscopy

Samples containing 8.4×10^{-5} M residues of $d(A\text{-}G)_{20}$ and $d(A\text{-}G)_{30}$ in buffer were heated to 40–50°C, cooled slowly and incubated for 10 min at the desired temperature prior to measurement of CD. For melting profiles, CD spectra from 320 to 220 nm between 2 and 60°C were recorded every 6°C on a computer-driven AVIV 62DS CD spectrometer equipped with a thermoelectrically-controlled cell holder. Digitized data obtained every 1 nm were corrected for baseline at the ambient temperature and smoothed by a least-squares polynomial fit up to the third order. CD spectra per mole of monomer are plotted as Δε in units of l/mol/cm. Profile reproducibility was excellent after several weeks storage of samples at –20°C.

UV spectroscopy

Absorption spectra and thermal melting profiles were measured with a computer-driven AVIV 14DS spectrophotometer equipped with a thermoelectrically-controlled cell holder. For melting experiments, data were taken as spectra measured between 320 and 220 nm at 1 nm intervals every 2°C and converted to melting profiles at desired wavelengths. T_m was determined as the maximum of the differentials (dA/dT versus T) of the profiles.

Gel electrophoresis under non-denaturing conditions

Samples of $d(A\text{-}G)_{20}$ and $d(A\text{-}G)_{30}$ at pH 5.0 in 0.001, 0.01 and 0.21 M Na^+ and varying in concentration from 2.6×10^{-6} to 2.1×10^{-3} M (residues) were heated [duplex standards to 85°C, $d(A\text{-}G)_{20}$ and $d(A\text{-}G)_{30}$ to 50°C], cooled slowly to 25°C and then equilibrated at 4°C overnight. The duplex and triplex size markers, each 1×10^{-4} M (residues), were similarly treated. $d(A\text{-}G)_{20}$, $d(A\text{-}G)_{30}$ and the 41mer were each 5′-^{32}P-end-labeled and purified (13) and an equal amount of each was used to label appropriate samples. At 4°C, 4 µl aliquots were added to 1 µl loading dye [15% Ficoll type 400 (Pharmacia), 0.25% bromophenol blue, 0.25% xylene cyanol in H_2O], mixed briefly and loaded onto a pre-electrophoresed 12% native polyacrylamide gel. Gel and circulating electrophoresis buffers contained 1 mM EDTA in addition to 0.01 or 0.21 M Na^+, all titrated to the desired pH with acetic acid. Gels were run at 25–28 V/cm at 4°C with recirculation. For autoradiography, X-ray film was exposed to wet gels for 8–12 h at 4°C.

Chemical modification with dimethylsulfate (DMS)

Reaction mixtures containing 1×10^{-4} M residues of 5′-^{32}P-labeled $d(A\text{-}G)_{20}$ or $d(A\text{-}G)_{30}$ in 0.001, 0.01 or 0.21 M Na^+ buffered at pH 5.0 and 0.5% DMS (added as a 10% solution in ethanol) in a total volume of 20 µl were incubated for 40 min at 4°C. Samples of $d(A\text{-}G)_{20}\cdot 2[d(C\text{-}T)_{10}]$, $d(A\text{-}G)_{30}\cdot 3[d(C\text{-}T)_{10}]$ and $2[d(C\text{-}T)_{10}]$: $d(A\text{-}G)_{20}\cdot 2[d(C\text{-}T)_{10}]$ (1×10^{-4} M residues) containing [^{32}P]$d(A\text{-}G)_n$ oligomer were similarly treated. After incubation, 5 µl stop reagent (1.5 M Na^+, pH 5.2, 1 M β-mercaptoethanol, 250 µg/ml tRNA) at 0°C were added and the oligomer was precipitated with ethanol, redissolved in 0.3 M Na^+, pH 5.2, ethanol precipitated twice more, dried and digested with 1 M piperidine in H_2O for 30 min at 85°C. Samples were then twice evaporated and washed with H_2O, evaporated and mixed with loading dye (9 µl deionized 98% formamide, 10 mM EDTA, pH 8.0, 0.25% bromophenol blue in H_2O), heated to 90°C and analyzed on a 12% denaturing gel subjected to pre-electrophoresis. The percentage of full-length oligomer remaining at each time point was determined after autoradiography of wet gels and scintillation counting of cut bands of full-length oligomer and of digestion products. The results are corrected for baseline piperidine cleavage and expressed as percentage oligomer cleaved.

S1 nuclease digestion

Samples in a total volume of 30 µl contained 1×10^{-4} M 5′-^{32}P-labeled $d(A\text{-}G)_{20}$ in 0.001, 0.01 or 0.21 M Na^+ at pH 5.0 and $d(A\text{-}G)_{20}\cdot 2[d(C\text{-}T)_{10}]$ in 0.21 M Na^+ at pH 5.0 were treated with 0.017 U S1 nuclease at 4°C. Reaction was stopped by transferring 5 µl aliquots at 1, 2, 5, 10, 15 and 30 min to 4 µl loading dye (70% formamide, 0.1% bromophenol blue, 57 mM EDTA, pH 7.5) and freezing. Frozen samples were heated at 90°C for 2 min prior to loading on a pre-electrophoresed 12% denaturing gel and electrophoresis at 45 V/cm. The percent full-length oligomer remaining at each time point was determined after autoradiography of wet gels and scintillation counting of cut bands of full-length oligomer and of digestion products.

RESULTS

Acid-dependent duplex at low ionic strength

CD spectra of $d(A\text{-}G)_{20}$ and $d(A\text{-}G)_{30}$ in 0.001 M Na^+ (very low) and 0.01 M Na^+ (low) were measured between pH 3.5 and 6.0 at 3 and 25°C. Both oligomers display strong pH-dependence of CD intensity under these conditions, with the intense circular dichroism at lower pH characteristic of a helical structure. A representative plot of Δε versus λ_{nm} for $d(A\text{-}G)_{30}$ in 0.01 M Na^+ illustrates this dependence (Fig. 1A). The very significant decrease in intensity between pH 5.0 and 5.5 shows that a strongly chiral structure undergoes a major conformational transition as

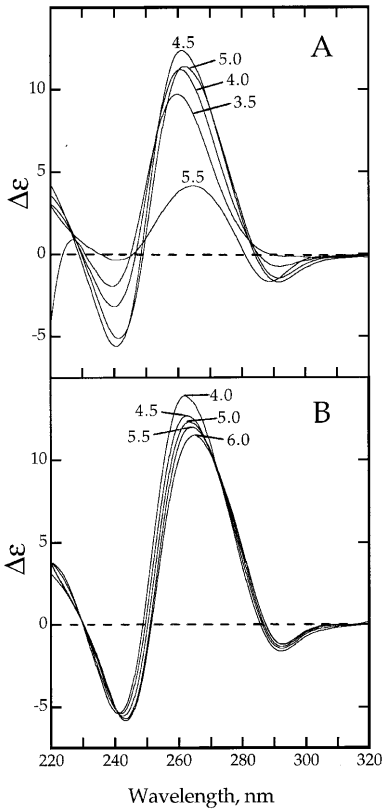

Figure 1. CD spectra for d(A-G)$_{30}$ at 3°C as a function of pH. (**A**) 0.01 M Na^+, pH 3.5–5.5; (**B**) 0.21 M Na^+, pH 4.0–6.0.

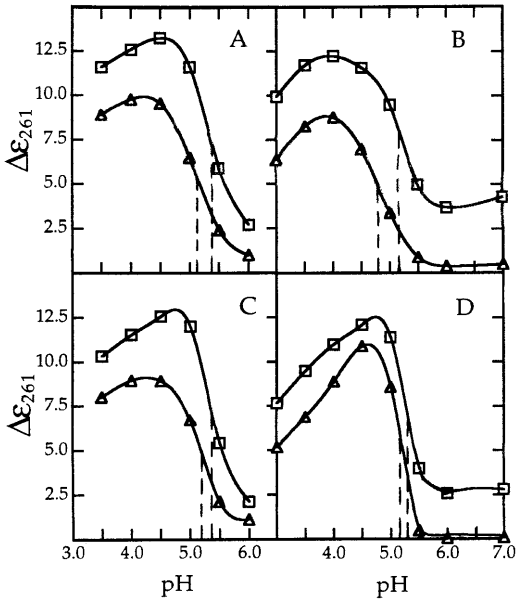

Figure 2. pH titration curves monitored by CD at 3°C (□) and 25°C (Δ). (**A**) d(A-G)$_{20}$ in 0.001 M Na^+; (**B**) in 0.01 M Na^+. (**C**) d(A-G)$_{30}$ in 0.001 M Na^+; (**D**) in 0.01 M Na^+. The dashed lines indicate extrapolated pK_a values.

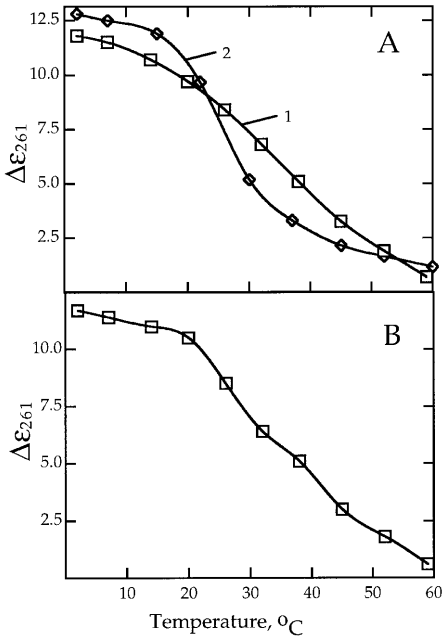

Figure 3. Melting profiles monitored by CD. (**A**) d(A-G)$_{20}$ in 0.01 M Na^+, pH 4.0 (1) and in 0.001 M Na^+, pH 5.0 (2). (**B**) d(A-G)$_{30}$ in 0.01 M Na^+, pH 4.0.

pH rises in this range. The CD-monitored titration curves in Figure 2 show that the pK_a values for both lengths of oligomer drop on going from 3 to 25°C and as Na^+ is raised from 0.001 to 0.01 M.

In low Na^+ at pH 4.0, a broad CD melting profile is observed for d(A-G)$_{20}$ like that for the α-helix of d(A-G)$_{10}$ (cf. Fig. 3A, curve 1, with figs 6 and 7A in ref. 11). However, between pH 4.5 and 5.5 in very low and low Na^+, the CD melting profiles for both oligomers show an abrupt (cooperative) transition reflecting the disruption of stacked bases presumably in a duplex (see for example Fig. 3A, curve 2). In this connection, it is instructive that at pH 4.0 in low Na^+, d(A-G)$_{30}$ undergoes biphasic melting (Fig. 3B), apparently because this pH and ionic strength represent boundary conditions for the transition between a cooperatively melting, base stacked structure at low temperature and the α-helix at somewhat higher temperature.

Given that the much more cooperative melting observed by CD for acid-dependent d(A-G)$_{20}$ and d(A-G)$_{30}$ distinguishes them from the α-helix, it is of interest to compare their UV melting characteristics as well. Like the α-helix, d(A-G)$_{20}$ at pH 4.0 and d(A-G)$_{30}$ at pH 3.5 in very low Na^+ show little hypochromicity and non-cooperative melting (see for example Fig. 4). This shows that the longer oligomers can also form the single-stranded α-helical structure characterized for d(A^+-G)$_{6,10}$. However, at pH ≥ 4.0, the longer chains undergo a transition from α-helix to a base stacked, acid-dependent putative duplex (see below). Thus, at pH 4.5 and above both oligomers show a large cooperative hyperchromic change on melting. This indicates a structure, different from the α-helix, that is most stable at pH 5.0 in very low salt for both oligomer lengths (Fig. 5). With T_m values at 260 nm of 23.5°C for d(A-G)$_{20}$ and 33.4°C for d(A-G)$_{30}$, it is apparent that increasing length favors the structure.

UV melting profiles for d(A-G)$_{20}$ and d(A-G)$_{30}$ in low Na^+ over the same pH range give similar results (not shown), although the cooperatively melting structure is most stable under more acidic conditions (pH 4.5) than in very low Na^+ (pH 5.0) (Fig. 5). Consistent with this, the higher ionic strength suppresses stability,

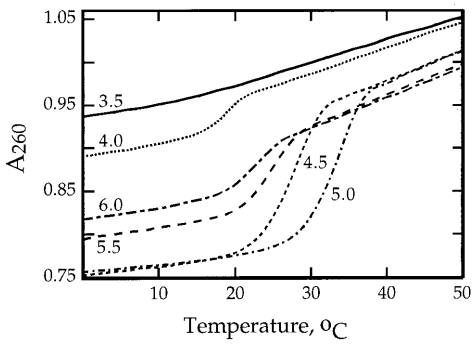

Figure 4. UV melting profiles for d(A-G)$_{30}$ in 0.001 M Na^+ between pH 3.5 and 6.0.

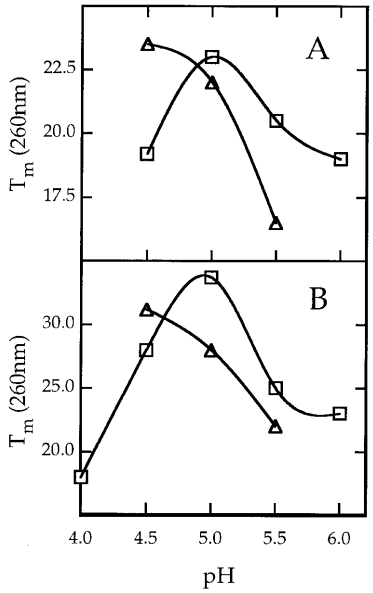

Figure 5. Melting temperatures for duplexes formed by d(A-G)$_{20}$ (**A**) and d(A-G)$_{30}$ (**B**) as a function of pH in 0.001 M Na^+ (□) and 0.01 M Na^+ (Δ).

e.g., the T_m at 260 nm for d(A-G)$_{30}$ is 30.9°C in low Na^+ but 33.4°C in very low Na^+ (Fig. 5B), though for d(A-G)$_{20}$ these values are nearly the same, 23.5 and 24.1°C respectively (Fig. 5A). UV melting profiles at 280 nm follow these trends, although T_m values at this wavelength, which is specific for dG residues, are consistently 1–2°C *lower* than those at 260 nm (see below).

An increase in Na^+ concentration can have three possible effects: (i) by shielding backbone phosphates, it can make it more favorable for two homopurine strands to come within base pairing distance; (ii) it can thereby also weaken any ionic attractions of phosphates for protonated adenines and consequently H-bonding between exocyclic amino hydrogens and the backbone phosphates; (iii) it can decrease the pK_a for protonation of dA residues. In fact, whereas an increase in ionic strength leads to greater stability of Watson–Crick duplexes, the opposite is observed with d(A-G)$_{30}$. On raising Na^+ from 0.001 to 0.01 M, T_m at the pH of maximum stability for the cooperative transition *decreases* by a few degrees (Fig. 5B). Thus, as in the α-helix, electrostatic attractions between protonated dA residues and phosphate groups are indicated in the pH-dependent stacked base pair structure that contribute more to

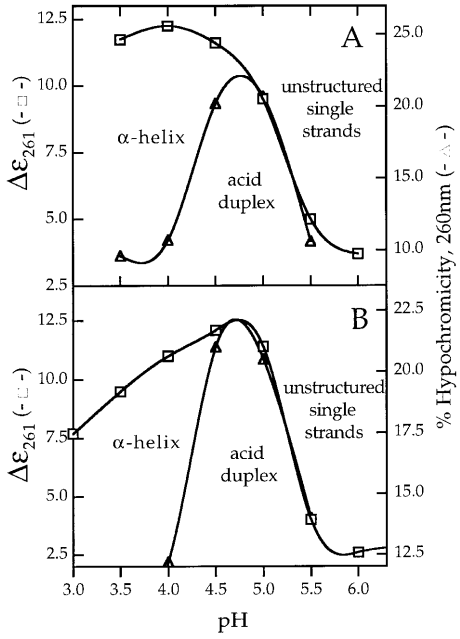

Figure 6. Superposition of pH titration curves monitored by CD (□) and UV hypochromicity at 260 nm ($A_{max} - A_{min}/A_{max}$) as a function of pH (Δ) for d(A-G)$_{20}$ (**A**) and d(A-G)$_{30}$ (**B**) in 0.01 M Na^+ at 3°C.

helix stability than does reduction of backbone strand repulsion. In the case of the shorter d(A-G)$_{20}$ oligomer, these opposing effects must be nearly the same (Fig. 5A).

By superimposing plots of CD intensity and UV hypochromicity as a function of pH (Fig. 6), three pH zones are delineated: a left zone, characterized by intense CD and marginal hypochromicity, in which the α-helix prevails; a middle zone, characterized by intense CD matched by strong hypochromicity, in which the putative duplex prevails; a right zone, with both weak CD and hypochromicity, in which the oligomers are unstructured single strands. Around the boundary at pH 4.3 there is an equilibrium mixture of α-helix and putative duplex, while at the boundary around pH 5.3 the equilibrium is between duplex and unstructured oligomer. The differences between Figure 6A and B indicate that the tendency to form the α-helix is reduced with increasing length of oligomer, possibly because the number of residues available for cooperative interstrand base pairing is increased. In line with this, d(A-G)$_{10}$ forms only the α-helix and no multistranded structure under the same conditions. This suggests that a minimum number of repeating units, $10 < n < 20$, is necessary for acid duplex formation.

It should be noted that some samples demonstrated variability in the amount of hyperchromic change with successive melts in very low and low Na^+. Just as there is an equilibrium between the α-helix and acid-dependent duplex in the pH-boundary region, so must there be one at constant pH in the salt range between 0.001 and 0.01 M; and very slight shifts in salt concentration apparently drive formation of one or the other structure. In addition, there are indications of some hysteresis that may be due to time delay for nucleation of the duplex structure. To circumvent such problems, UV melts of d(A-G)$_{20}$ and d(A-G)$_{30}$ were conducted in somewhat more concentrated (0.015 M) Na^+ between pH 4.0 and 5.5. UV and CD melting profiles (not shown) of both oligomers

then showed reproducible cooperative transitions over this pH range, with maximum stability near pH 4.5 and T_m (260 nm) values of 25 and 34°C for d(A-G)$_{20}$ and d(A-G)$_{30}$ respectively. These results confirm the occurrence of the pH-dependent putative duplex.

pH-independent duplex at moderate ionic strength

On increasing the ionic strength to 0.21 M Na^+ (moderate), the acid-dependence of duplex formation is greatly diminished. Thus, titration monitored by CD does not reveal a pH-dependent transition (Fig. 1B). The small decrease and redshift of $\Delta\varepsilon_{max}$ represented by the family of CD spectra with three isosbestic points in Figure 1B probably reflects a decrease in the degree of protonation of the dA residues as the pH is raised. But this decrease is not attended by a conformational transition, as is evident in 0.01 M Na^+ (Fig. 1A). The contrasting pH-dependencies in low and moderate Na^+ are suggestive of different sources of helix stability, as are the contrasting ionic strength dependencies of stability (see below). Nevertheless, the pH-independent duplexes in 0.21 M Na^+ do undergo cooperative melting with large CD and UV absorbance changes (data not shown). These duplexes show only slight T_m maxima at pH 4.5 in both cases and complete pH-independence above pH 5.5 (Table 1), where dA residues are no longer protonated. Consistent with such behavior, this structure shows *positive* ionic strength dependence of melting at pH 6 not unlike that for DNA duplexes of similar length, with $dT_m/d\log[Na^+]$ = ~18°C.

Table 1. T_m of duplexes formed by d(A-G)$_{20,30}$ in 0.21 M Na^+ as a function of pH

pH (± 0.1)	T_m (°C ± 0.1)	
	d[(A-G)$_{20}$·(A-G)$_{20}$]	d[(A-G)$_{30}$·(A-G)$_{30}$]
4.0	46.0	51.7
4.5	47.1	52.0
5.0	45.0	50.0
5.5	43.5	47.9
6.0	43.1	47.4
7.0	43.0	47.3
7.5	43.3	47.4
8.0	43.4	47.2

Figure 7 shows CD spectra measured on samples of d(A-G)$_{30}$ under different conditions that are believed to stabilize the three conformations discussed here for d(A-G)$_n$, i.e., the α-helix (spectrum 1), the acid-dependent putative duplex (spectrum 2) and the pH-independent putative duplex (spectrum 3). Although all three structures are characterized by intense circular dichroism, it is apparent that their CD spectra are unique.

Contrasting effects of ethanol on the two types of duplex

To further characterize the interactions that contribute predominantly to stabilization of the acid-dependent and pH-independent duplexes, the effect of ethanol on T_m was examined. Lowering the dielectric constant is known to stabilize electrostatic interactions, but to weaken base stacking due to enhanced base solvation. On going from 0 to 5% ethanol in 0.01 M Na^+ at pH 5.0, the T_m of

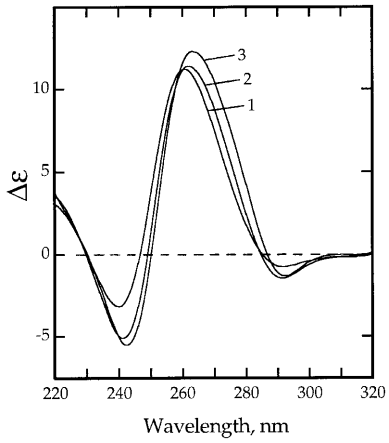

Figure 7. CD spectra for three different structures formed by d(A-G)$_{30}$ at 3°C: (1) α-helix in 0.01 M Na^+, pH 4.0; (2) acid-dependent duplex in 0.01 M Na^+, pH 5.0; (3) pH-independent duplex in 0.21 M Na^+, pH 5.0.

d(A-G)$_{20}$ *increases* from 21.8 to 24°C, confirming that ionic interaction between protonated dA residues and the PO_2^- of the backbone phosphate moieties contribute significantly to stabilization of the acid-dependent duplex. In contrast, T_m values *decrease* for the pH-independent duplex formed by d(A-G)$_{20}$ in 0.21 M Na^+ at pH 5.5, from 43.8 to 42.8 and then to 41.4°C in the presence 0, 5 and 10% ethanol respectively. This effect is as observed for Watson–Crick duplexes, which have no interstrand ionic attractions.

Strandedness of acid-dependent and pH-independent helices

Indications that the acid-dependent and pH-independent structures are multistranded were first obtained from the observation of a concentration-dependence of T_m values provided by UV melting profiles. For d(A-G)$_{20}$ at pH 4.5 in 0.01 M Na^+ and at pH 5.0 in 0.21 M Na^+, 10-fold increases in oligomer concentration raise the T_m value from 23.8 to 26°C and from 45.1 to 47.8°C respectively, and a similar concentration dependence of thermal stability was observed for d(A-G)$_{30}$. Strandedness was more directly examined by native gel-mobility assays. In running buffer with 0.01 M Na^+ at pH 5.0, d(A-G)$_{20}$ incubated in 0.001 and 0.01 M Na^+ migrates essentially the same as the 41 bp Watson–Crick duplex size marker (Fig. 8) and d(A-G)$_{30}$ migrates as expected for a 60 bp duplex, i.e., with proportionately slower mobility than the 41mer duplex marker. Electrophoretic mobilities of d(A-G)$_{20}$ and d(A-G)$_{30}$ were also examined over a 1000-fold oligomer concentration range, from 5×10^{-6} to 1×10^{-3} M in 0.01 M Na^+, pH 5.0. At very low oligomer concentration, trace amounts of single strands of d(A-G)$_{20}$ but not of d(A-G)$_{30}$ are present, showing that there is an equilibrium between the single-strand α-helix and the duplex formed by the shorter oligomer.

Comparable experiments on gels with oligomers incubated in 0.21 M Na^+ at pH 5.0 were performed using the same moderate ionic strength running buffer. At this Na^+ concentration d(A-G)$_{20}$·2[d(C-T)$_{10}$] and d(A-G)$_{30}$·3[d(C-T)$_{10}$] form stable 40 and 60 bp duplex markers respectively (not shown). Over a 1000-fold range of oligomer concentration, d(A-G)$_{20}$ and d(A-G)$_{30}$ have mobilities comparable with the corresponding Watson–Crick duplexes, indicating homopurine·homopurine duplex formation in moderate salt. These native PAGE analyses

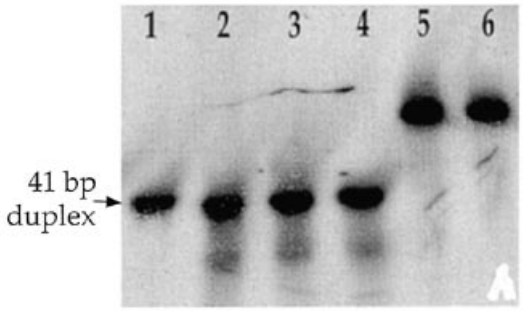

Figure 8. Native gel electrophoretic assays for complexes formed by $d(A\text{-}G)_{20}$ and $d(A\text{-}G)_{30}$ at pH 5.0, 4°C. Gels are 12% polyacrylamide; running buffer 0.01 M Na^+, 1 mM EDTA, pH 5.0. Variations in [Na^+]: lane 1, 41 bp control duplex incubated in 0.01 M Na^+; lane 2, $d(A\text{-}G)_{20}$ incubated in 0.001 M Na^+; lane 3, in 0.01 M Na^+; lane 4, in 0.015 M Na^+; lane 5, $d(A\text{-}G)_{30}$ incubated in 0.001 M Na^+; lane 6, in 0.01 M Na^+. For both oligomers, $c \approx 1 \times 10^{-4}$ M (residues). A 41mer marker was employed because $d(A\text{-}G)_{20}$ does not form a duplex with $d(C\text{-}T)_{10}$ at pH 5.0 in 0.01 M Na^+ due to preferred duplex formation by $d(C^+\text{-}T)_{10}$ (16).

confirm the double-strandedness of the acid-dependent and pH-independent duplexes.

H-bonding schemes for the duplexes

In attempting to deduce H-bonding schemes for the two types of duplex, we considered antiparallel versus parallel strand orientation and homo versus hetero base pairs (Fig. 9). When both members of the pair are in antiparallel strands, one of the two bases in A·A and G·G base pairs must be an unfavored tautomer (pairs 1 and 2) (17), but this is energetically intolerable when such pairs are present in the duplex in high frequency. The hetero pair $G_{anti}\cdot A_{anti}$ (18) may be dismissed for the acid-dependent duplex because protonation of A is prohibited by the involvement of N1 of A as a hydrogen acceptor (pair 3); and while such a scheme is conceivable for the neutral *anti·anti* pair, the smooth and instantaneous transition of acid duplex to neutral duplex makes it unlikely. For energetic reasons, a full complement of $G_{anti}\cdot A_{syn}$ pairs with the A residues protonated or neutral (pair 4) (8,19) seems unlikely. In fact, this pairing scheme has been shown to occur for $d(A\text{-}G)_n$ only when forced in a hairpin duplex stabilized by a long run of flanking Watson–Crick pairs (8,9). Finally, protonated $A_{anti}\cdot G_{syn}$ pairs (pair 5) (20) are ruled out by the unavailability of N7 of dG residues for reaction with DMS (see below).

Against this background of contra-indications for antiparallel-stranded duplexes, there are several indications for A·A and G·G base pairs within parallel strands, especially for the acid-dependent duplex in which the dA residues are protonated and involved in base–backbone interactions of the same type as present in the poly($A^+\cdot A^+$) duplex (pair 6) (21,22). This requires a compatible G·G pair, for which there are two possibilities, one with the two residues *syn* (pair 7) (5) and the other with both residues *anti* (pair 8) (6). While both these combinations of A·A and G·G pairs have been suggested for parallel-stranded duplexes with the alternating $(A\text{-}G)_n$ sequence, the evidence from NMR spectroscopy (6) would seem to be much more compelling than the indirect evidence from circular dichroism. In the NMR structure, while the backbone linkages between the two types of homopairs are

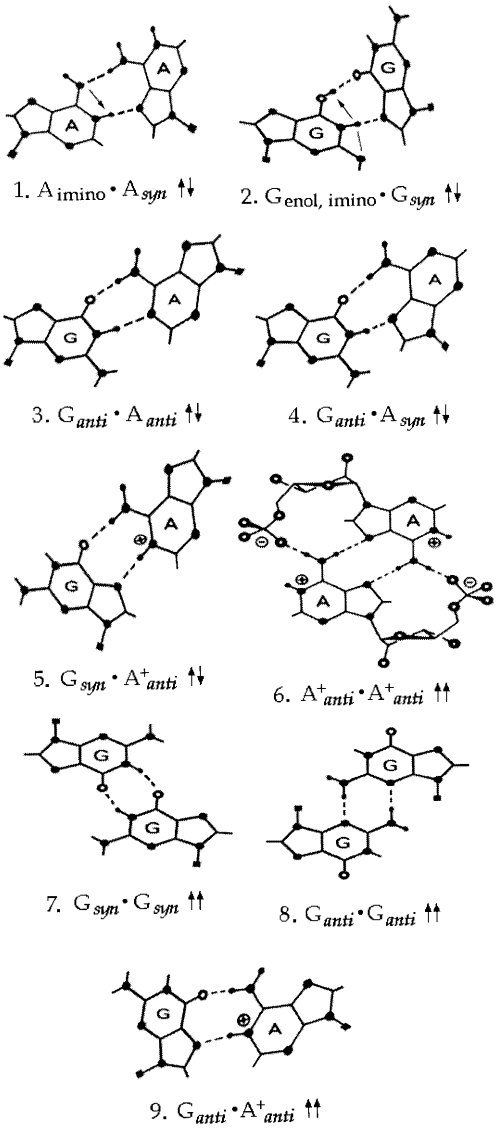

Figure 9. Some alternative base pairing schemes for homoduplexes of $d(A^+\text{-}G)_n$ and $d(A\text{-}G)_n$. For clarity, double bonds are not shown; arrows indicate where tautomerism has shifted hydrogen positions.

novel, resulting in a 2-bp stereochemical repeat, the stereochemistry of the base pairs themselves is not. All residues are oriented *anti* about the glycosyl bonds and the protonated adenines are H-bonded to the backbone P=O, as would be expected if the ionic attractions between their $N1H^+$ moieties and the backbone PO_2^- were in force as well.

An alternative possibility for parallel strands in acid solution involves a $G\cdot A^+$ base pair (pair 9) (5). However, this scheme does not allow for the base–backbone ionic interaction indicated by the observed sensitivity to ionic strength. In this hetero base pair, the pH–sensitive H-bond involves N7 of dG and $N1H^+$ of dA residues.

To further distinguish between the most likely hetero pair and alternating homo base pairing schemes in the two types of duplex, DMS was used to probe the accessibility of N7(dG) to methylation. The extent of cleavage of $d(A\text{-}G)_{20}$ and $d(A\text{-}G)_{30}$ in 0.001, 0.01 and 0.21 M Na^+ at pH 5.0 is compared with that for Watson–Crick duplexes and the corresponding triplex of

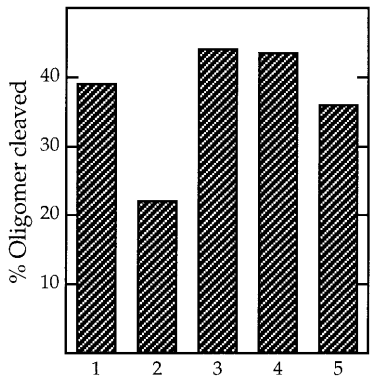

Figure 10. The percentage of oligomer cleaved by piperidine after chemical modification of d(A-G)$_{20}$ with DMS at pH 5.0 in various complexes and ionic conditions. (1) Control duplex d(A-G)$_{20}$·2[d(C-T)$_{10}$] in 0.21 M Na^+; (2) control triplex d(A-G)$_{20}$·4[d(C-T)$_{10}$] in 0.21 M Na^+; (3) d(A-G)$_{20}$ in 0.21 M Na^+; (4) in 0.01 M Na^+; (5) in 0.001 M Na^+. Data were corrected for piperidine cleavage of unmodified oligomer. The results are averages of three experiments.

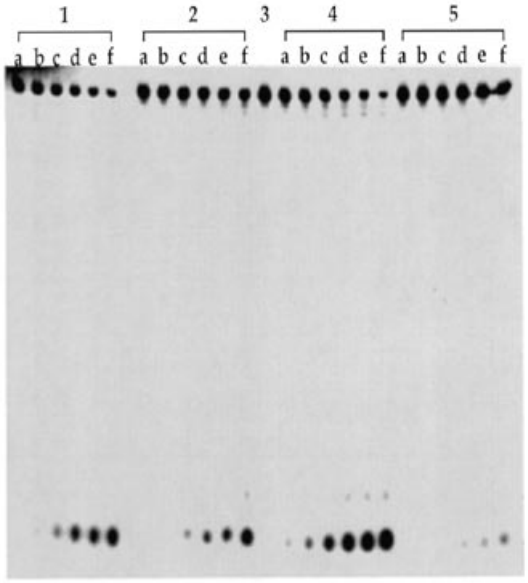

Figure 11. Assay on 12% denaturing polyacrylamide gel of S1 cleavage products at pH 5.0, 4°C. (1) Control duplex d(A-G)$_{20}$·2[d(C-T)$_{10}$] in 0.21 M Na^+; (2) d(A-G)$_{20}$ in 0.21 M Na^+; (3) d(A-G)$_{20}$ undigested control in 0.01 M Na^+; (4) d(A-G)$_{20}$ in 0.01 M Na^+; (5) d(A-G)$_{20}$ in 0.001 M Na^+. Reaction times a–f are 1, 2, 5, 10, 15 and 30 min respectively.

d(A-G)$_{20}$ with a homopyrimidine third strand in moderate ionic strength (Fig. 10). It is apparent that the triplex structure (bar 2), in which Hoogsteen base pairing should protect N7(dG) from DMS methylation, has a low percentage of cleaved oligomer, while the Watson–Crick, acid-dependent and moderate salt duplexes for both oligonucleotides all show similarly higher levels of backbone cleavage by piperidine. These results indicate that, as in the Watson–Crick duplex, N7 of G is not involved in interbase H-bonding. Consequently, the two duplexes formed at all three ionic strengths are stabilized by A^+·A^+/G·G (Fig. 9, pairs 6 and 8) or A·A/G·G rather than by G·A^+ (pair 9) base pairs.

S1 nuclease digestion

To distinguish between hairpin and linear structures, 5′-^{32}P-labeled d(A-G)$_{20}$ at pH 5.0 in 0.001, 0.01 and 0.21 M Na^+ was digested with S1 nuclease. A Watson–Crick d(A-G)$_{20}$·2[d(C-T)$_{10}$] duplex in 0.21 M Na^+ at pH 5.0 served as a duplex standard. Electrophoresis on a denaturing gel revealed very small amounts of the $n-1$, $n-2$ and corresponding mono- and dinucleotide products, presumably due to fraying of the ends of the duplexes, but *none of the intermediate size fragments* which would result from random cleavage of a single-stranded structure or the half-molecule fragments expected from cleavage of a hairpin turn (cf. 7). This general resistance of both types of d(A-G)$_{20}$ duplex to endonuclease cleavage is like that of the Watson–Crick duplex and shows that the structures formed in very low, low and moderate Na^+ do not contain hairpin turns (Fig. 11). Moreover, the efficacy of the enzyme for cleaving single strands preferentially at pH 5.0 at all three Na^+ concentrations was confirmed using a non-repetitive single-stranded 35mer and its Watson–Crick duplex (data not shown).

It is interesting that the control duplex d(A-G)$_{20}$·2[d(C-T)$_{10}$] is digested faster than the d(A-G)$_{20}$ duplex at 0.001 and 0.21 M Na^+. Conceivably, this is because the phosphodiester bonds in the Watson–Crick duplex are more accessible to the enzyme than in the homopurine duplex. At pH 5.0, the dA^+–backbone interactions probably close the major groove, much as in the poly(A^+·A^+) duplex (21,22).

DISCUSSION

The pH-dependence of the helical structure at 0.001 and 0.01 M Na^+ indicates that protonation of most dA residues is essential to the stability of the acid-dependent d(A^+-G)$_{20,30}$ duplexes, since cooperative melting and hypochromism disappear near pH 5.5. In contrast, the structure in moderate salt depends little on protonation of dA residues for stability, its structure extending well into the neutral pH range with almost no diminution in T_m value.

What must distinguish the duplexes stabilized below 0.02 M Na^+ and above 0.2 M Na^+ is the relative significance of the base–backbone interactions. At low ionic strength and pH, these interactions are the dominant cohesive ones; but with more effective charge shielding and reduction of the fraction of dA residues that are protonated at pH values much above their intrinsic pK_a, the dA^+–backbone interactions are substantially diminished and weakened. Consequently, while the two types of duplex share the same interbase H-bonding, the ionic and H-bonds between dA^+ and the backbone, which are associated because of the hybrid character of PO_2^-, probably alter the helical twist of the two strands, so that the structure of the grooves in the two cases must be different. This must be what largely accounts for the difference between the CD spectra of the two duplex forms at pH 5.0 shown in Figure 7.

It is interesting that poly(A^+·A^+), which has the same base–backbone interactions as the d(A^+·A^+) base pairs in the d(A^+-G)$_{20,30}$ duplexes, does not survive at neutral pH (23). If it did, the interbase A·A H-bonding would be as in the d(A-G)$_{20,30}$ linear duplexes, stable at neutrality in moderate to high salt (data not shown). We take this difference in pH-sensitivity to mean that the neutral duplexes of d(A-G)$_{20,30}$ derive their unique stabilization from the alternating presence of the G·G base pairs, which NMR

and model building studies (6) have shown to stack especially well with their cross-strand nearest-neighbor dA residues.

It is also worth noting that at the higher cation concentrations where the pH-independent duplex is stable, the ionic bond-stabilized α-helix does not form at even the most optimal acidic pH. This emphasizes the similarity between the base–backbone interactions of the nucleic acid α-helix and the acid-dependent duplex, as well as the differences between the two types of helix. Although the single-stranded structure lacks the stabilization that comes from stacking of base pairs, stacking that becomes increasingly advantageous for the duplex with greater strand length, the single-stranded structure is preferred entropically for very short strands, because of the much greater ease of intra- than intermolecular nucleation.

The biological relevance of the $d(A\text{-}G)_n$ sequences in mammalian genomes is not illuminated by the occurrence of the pH-independent parallel duplex with A·A and G·G base pairs. However, it does suggest, as we have indeed found, that irregular sequences of dA and dG residues form duplexes, presumably with irregular sequences of A·A and G·G base pairs. This must be why some homopurine sequences do not serve effectively as third strands for triplex formation.

ACKNOWLEDGEMENTS

This work was supported by NIH grant GM 42936 to J.R.F. and a Fellowship from Oncor Inc. to N.G.D.

REFERENCES

1 Hoffman,E.K., Trusko,S.P., Murphy,M. and George,D.L. (1990) *Proc. Natl. Acad. Sci. USA*, **87**, 2705–2709.
2 Reaban,M.E. and Griffin,J.A. (1990) *Nature*, **348**, 342–344.
3 Aharoni,A., Baran,N. and Manor,H. (1993) *Nucleic Acids Res.*, **21**, 5221–5228.
4 Kolluri,R., Torrey,A. and Kinniburgh,A.J. (1992) *Nucleic Acids Res.*, **20**, 111–116.
5 Rippe,K., Fritsch,V., Westhof,E. and Jovin,T.M. (1992) *EMBO J.*, **11**, 3777–3786.
6 Robinson,H., van Boom,J.H. and Wang,A.H.-J. (1994) *J. Am. Chem. Soc.*, **116**, 1565–1566.
7 Shiber,M.C., Braswell,E. H., Klump,H. and Fresco,J.R. (1996) *Nucleic Acids Res.*, **24**, 5005–5013.
8 Huertas,D., Bellsolell,L., Casasnovas,J.M., Coll,M. and Azorín,F. (1993) *EMBO J.*, **12**, 4029–4038.
9 Casasnovas,J.M., Huertas,D., Ortiz-Lombardía,M., Kypr,J. and Azorín,F. (1993) *J. Mol. Biol.*, **233**, 671–681.
10 Mukerji,I., Shiber,M.C., Fresco,J.R. and Spiro,T. (1996) *Nucleic Acids Res.*, **24**, 5013–5020.
11 Dolinnaya,N.G. and Fresco,J.R. (1992) *Proc. Natl. Acad. Sci. USA*, **89**, 9242–9246.
12 Dolinnaya,N.G., Braswell,E.H., Fossella,J.A., Klump,H. and Fresco,J.R. (1993) *Biochemistry*, **32**, 10263–10270.
13 Shiber,M.C., Lavelle,L., Fossella,J.A. and Fresco,J.R. (1995) *Biochemistry*, **34**, 14293–14299.
14 Mukerji,I., Shiber,M.C., Spiro,T.G. and Fresco,J.R. (1995) *Biochemistry*, **34**, 14300–14303.
15 Lee,J.S., Evans,D.H. and Morgan,A.R. (1980) *Nucleic Acids Res.*, **8**, 4305–4320.
16 Guschlbauer,W. (1967) *Proc. Natl. Acad. Sci. USA*, **57**, 1441–1448.
17 Topal,M.D. and Fresco,J.R. (1976) *Nature*, **263**, 285–289.
18 Privé,G.G., Heinemann,U., Chandrasegaran,S., Kan,L.-S., Kopka,M.L. and Dickerson,R.E. (1987) *Science*, **238**, 498–504.
19 Hunter,W.N., Brown,T. and Kennard,O. (1986) *J. Biomol. Struct. Dynam.*, **4**, 173–191.
20 Brown,T., Leonard,G.A., Booth,E.D. and Chambers,J. (1989) *J. Mol. Biol.*, **207**, 455–457.
21 Fresco,J.R. (1959) *J. Mol. Biol.*, **1**, 106–110.
22 Rich,A., Davies,D.R., Crick,F.H.C. and Watson,J.D. (1961) *J. Mol. Biol.*, **3**, 71–86.
23 Fresco,J.R. and Klemperer,E. (1959) *Annls NY Acad. Sci.*, **81**, 730–741.

This paper is no. 26 in the series entitled ‘Polynucleotides’, of which the last is Mukerji *et al.* (10).